

Melting Behavior of a Covalently Closed, Single-Stranded, Circular DNA<sup>†</sup>Dorothy A. Erie,<sup>†</sup> Roger A. Jones,<sup>‡</sup> Wilma K. Olson,<sup>‡</sup> Navin K. Sinha,<sup>§</sup> and Kenneth J. Breslauer<sup>\*‡</sup>*Department of Chemistry and Waksman Institute, Rutgers—The State University of New Jersey, Piscataway, New Jersey 08855-0939**Received May 25, 1988; Revised Manuscript Received August 16, 1988*

**ABSTRACT:** We synthesized the 26-residue deoxynucleotide sequence d(TTCCT<sub>5</sub>GGAATTCCT<sub>5</sub>GGAA) which folds intramolecularly to form a dumbbell-shaped, double-hairpin structure with a gap between the 3' and the 5' ends. We used T4 polynucleotide kinase to phosphorylate the 5' end followed by T4 DNA ligase to close the 3' and 5' ends. Melting of the dumbbell structure formed by this ligated sequence produces a covalently closed, single-stranded, circular final state. We employed calorimetric and spectroscopic techniques to characterize thermodynamically the melting behavior of the ligated molecule and compared it with the corresponding melting behavior of its unligated precursor. This comparison allowed us to characterize uniquely the influence of single-stranded ring closure on intramolecular duplex melting. The data reveal that ring closure produces a thermally more stable structure which exhibits significantly altered melting thermodynamics. We rationalize these thermodynamic differences in terms of differential solvation and differential counterion association between the ligated and unligated molecules. We also note the importance of such constrained dumbbell structures as models for hairpins, cruciforms, and locally melted domains within naturally occurring DNA polymers.

**D**NA secondary structures containing nonbonded regions appear to play important roles in biologically significant events, such as gene expression. Palindromic sequences provide one example of DNA domains which can self-anneal to form hairpins and/or cruciform structures. Such regions frequently occur in supercoiled DNAs (Lilley, 1986) and appear at or near loci of biological control in natural DNAs (Streisinger et al., 1966; Müller & Fitch, 1982), thereby suggesting a functional role for these secondary structures. Looped-out regions of DNA (e.g., bulges) also are believed to be important in biological processes such as transcription (Yager & von Hippel, 1987). In fact, the mechanisms of numerous biological processes evoke the presence and participation of DNA secondary structures containing nonbonded domains. In recognition of this fact, we and others (Scheffler et al., 1970; Baldwin, 1971; Germann et al., 1985; Wemmer & Benight, 1985; Erie et al., 1987; Benight et al., 1988) have used oligomeric sequences to model DNA secondary structures which melt to constrained final states. As part of our program, we recently synthesized a family of oligomeric sequences which were designed to form dumbbell-shaped, double-hairpin structures. Upon ligation, these dumbbells melt to covalently closed, single-stranded circles. Such molecules provide models not only for hairpins and cruciforms but also for other DNA secondary structures with looped-out regions (e.g., locally melted domains in natural DNAs). The overall design of these molecules also allows us to characterize uniquely the effect of loop closure on the thermodynamics of an order-disorder transition.

In a previous paper, we characterized thermodynamically the melting behavior of the 24-mer sequence TTCCT<sub>4</sub>GGAATTCCT<sub>4</sub>GGAA (Erie et al., 1987). We presented thermodynamic, spectroscopic, and electrophoretic evidence that this molecule folds back onto itself to form a dumbbell-shaped, double-hairpin structure with a gap between

the 3' and the 5' ends. Phosphorylation of the 5' end produced a nicked dumbbell structure which exhibited altered melting behavior. Salt-dependent melting studies suggested that this change was due to an electrostatically induced distortion of the phosphorylated dumbbell structure. We also intended to ligate the phosphorylated derivative to produce a structure that would melt to a covalently closed, single-stranded "circle". Unfortunately, all our ligation efforts failed.

We reasoned, at the time, that the corresponding 26-mer DNA sequence with five rather than four thymine residues in the hairpin loops may more readily ligate since the 5' and 3' ends should be better aligned for bond formation (Erie et al., 1987). This expectation now has been realized. We have successfully ligated the corresponding 26-mer sequence, TTCCT<sub>5</sub>GGAATTCCT<sub>5</sub>GGAA. This ligation reaction produces a unique structure that allows us to characterize thermodynamically the melting of a duplex to a covalently closed, circular, single-stranded final state. Because of our experimental design, we can compare these results directly to the nicked precursor. Such a comparison enables us to characterize thermodynamically, for the first time, the effect of single-stranded ring closure on intramolecular DNA duplex melting. In this paper, we report the results of this investigation.

## MATERIALS AND METHODS

**Oligomers.** The unphosphorylated 26-mer initially was purchased from Pharmacia and was purified by reversed phase HPLC as described below. Subsequently, it was synthesized by employing the H-phosphonate method and purified as described previously (Gaffney & Jones, 1988).

**Phosphorylation.** Solutions of 5–100 nmol of 26-mer ([oligomer] = 5–100  $\mu$ M) in 70 mM Tris-HCl (pH 7.4), 10 mM MgCl<sub>2</sub>, 300  $\mu$ M rATP, and 1 mM dithiothreitol (DTT) were incubated at 37 °C with T4 polynucleotide kinase (1 unit/nmol of oligomer, Bethesda Research Laboratories, Bethesda, MD). After 60 min, a 2-fold excess of kinase and rATP was added. After an additional 120 min, the reaction was terminated by heating the mixture for 10 min at 65 °C. The extent of phosphorylation was monitored on a Perkin-

<sup>†</sup> This work was supported by NIH Grants GM20861, GM23509, GM24391, GM31483, and GM34469, American Cancer Society Grant CH248B, and the Charles and Johanna Busch Memorial Fund.

<sup>‡</sup> Department of Chemistry.

<sup>§</sup> Waksman Institute.

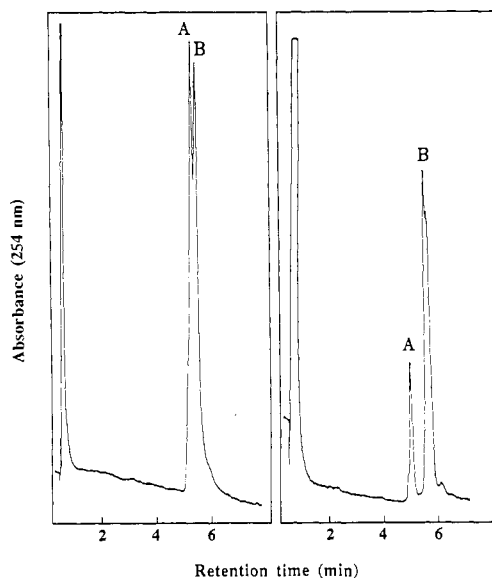


FIGURE 1: (Left panel) Reverse-phase HPLC chromatogram of a typical phosphorylation reaction mixture at approximately 50% completion. The gradient is 2–20% acetonitrile/0.1 M TEAA in 7 min at 3 mL/min. Peak A corresponds to the starting material and peak B to the phosphorylated material. (Right panel) Reverse-phase HPLC chromatogram of a ligation reaction mixture under the same conditions as above. Peak A corresponds to the ligated material and peak B to the starting material.

Elmer 410 BIO HPLC equipped with a Beckman C<sub>3</sub> column. A chromatogram of the reaction mixture at approximately 50% completion is shown in the left panel of Figure 1. Peak A corresponds to the starting material and peak B to the phosphorylated material. In all cases, phosphorylation was quantitative.

**Ligation.** After the above reaction mixture was cooled, rATP and DTT were added such that their final concentrations were 1 mM and 5 mM, respectively. T4 DNA ligase at a concentration of 1 unit/nmol of oligomer was added to this reaction mixture. All ligation reaction mixtures contained approximately 15% poly(ethylene glycol) (PEG) (Pheiffer & Zimmerman, 1983; Zimmerman & Pheiffer, 1983). The ligation reactions were carried out at 37 °C for 12–96 h. The extent of ligation was assayed by reversed-phase HPLC. A chromatogram of a ligation reaction mixture is shown in the right panel of Figure 1. The material corresponding to peak A was found to be resistant to degradation by several exonucleases (T4 polymerase,  $\lambda$  exonuclease, Exo III) and to dephosphorylation by alkaline phosphatase. Peak B of the chromatogram in the right panel of Figure 1 corresponds to the starting material. The yields of the ligation reactions ranged from 30 to 50%.

**Purification.** All purifications were carried out on a Perkin-Elmer 410 BIO HPLC system using a semipreparative Beckman Ultrapore C<sub>3</sub> column (1 × 25 cm) with a gradient of 2–20% CH<sub>3</sub>CN/0.1 M TEAA in 30 min at 3 mL/min. The fractions were analyzed on an analytical Beckman Ultrapore C<sub>3</sub> column using a gradient of 2–20% CH<sub>3</sub>CN/0.1 M TEAA in 7 min at 3 mL/min. The purified products were homogeneous when chromatographed as described above.

**Exonuclease Assays.** All exonuclease assays were performed at 37 °C for 30 min. The conditions for the T4 polymerase and Exo III assays were 33 mM Tris-acetate (pH 7.8), 10 mM MgAc<sub>2</sub>, 66 mM KAc, 100  $\mu$ g/mL nuclease-free bovine serum albumin, and 0.5 mM DTT. The conditions for the  $\lambda$  exonuclease assays were 1 mM DTT, 3 mM MgAc<sub>2</sub>, and 67 mM glycine (pH 9.4). The alkaline phosphatase assays

were performed in 10 mM Tris-acetate at 65 °C for 30 min. The reactions were monitored by reversed-phase HPLC as described above.

**Calorimetry.** The change in heat capacity for the thermally induced, order-disorder transition of the 26-mer was measured as a function of temperature on a Microcal 2 differential scanning calorimeter (Microcal, Amherst, MA). The calorimetric experiments were carried out in a pH 7 buffer containing 0.1 mM EDTA and 1.0 mM sodium phosphate buffer. The oligomer concentration was 122  $\mu$ M in single strands. The details of the calorimetric measurements and the data analysis have been described previously (Breslauer et al., 1975; Marky et al., 1983; Breslauer, 1986; Marky & Breslauer, 1987).

**Circular Dichroism (CD) Spectroscopy.** CD spectra were recorded on a Model 60DS AVIV spectropolarimeter (Lakewood, NJ) equipped with a thermoelectrically controlled cell holder. All solutions contained 1.0 mM phosphate buffer (pH 7.0), 0.1 mM EDTA, and various concentrations of NaCl (0.0–0.3 M). CD spectra were obtained at several temperatures ranging from 10 to 90 °C.

**Ultraviolet (UV) Spectroscopy.** Absorbance versus temperature profiles were measured at 260 nm on a Perkin-Elmer 575 spectrophotometer interfaced to a Tektronix 4051 computer. Melting profiles were obtained by increasing the temperature from 0 to 100 °C at a constant rate of 1.0 °C/min with a programmable, thermoelectrically controlled cell holder. Oligomer concentrations ranged from 0.6 to 122  $\mu$ M. These concentrations were determined spectroscopically from extinction coefficients calculated by the nearest-neighbor method (Cantor et al., 1970). The melting studies also were performed over a range of added salt concentrations from 0.0 to 1.0 M NaCl. All solutions contained 0.1 mM EDTA and 1.0 mM sodium phosphate buffer (pH 7.0). van't Hoff transition enthalpies ( $\Delta H_{vH}$ ) were determined from these optical melting curves according to previously described protocols [Breslauer et al., 1975; Marky et al., 1983; Breslauer (1986) and references cited therein; Erie et al., 1987].

**Analysis of the Salt-Dependent Melting Data.** As noted above, UV melting profiles were determined over a broad range of sodium ion concentrations (0.002–1.0 M). The corresponding thermodynamic data were obtained by evaluating the shape of each experimental melting curve by the previously described methods [Breslauer et al., 1975; Marky et al., 1983; Breslauer (1986) and references cited therein; Erie et al., 1987]. These data ( $\Delta H_{vH}$ ,  $T_m$ , and  $\partial T_m / \partial \log [Na^+]$ ) then were used to calculate the change in the thermodynamic degree of ion dissociation,  $\Delta i$ , for each transition at each salt concentration from

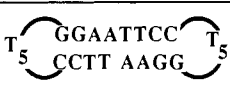
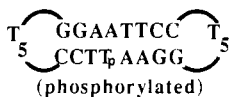
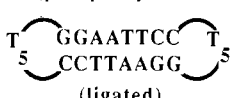
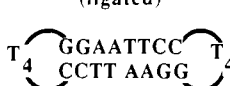
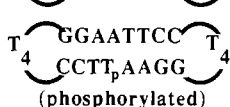
$$\frac{\partial T_m}{\partial \log [Na^+]} = \left( \frac{2.3RT_m^2}{\Delta H'_{vH}} \right) \Delta i \quad (1)$$

where  $T_m$  is the melting temperature,  $[Na^+]$  is the sodium ion concentration,  $\Delta H'_{vH}$  is the enthalpy change per phosphate, and  $\Delta i$  is the change in the degree of ion dissociation per phosphate upon denaturation (Record et al., 1978). This procedure has been described in detail previously (Erie et al., 1987). The  $\Delta i$  values listed in Table I are averaged over added salt concentrations between 0.0 and 0.3 M NaCl, thereby restricting our attention to the appropriate domain in which the  $T_m$  exhibits a linear dependence on  $\log [Na^+]$ .

## RESULTS

**CD Spectroscopy.** The overall shapes of the wavelength-dependent CD spectra for the unphosphorylated (I), phosphorylated (II), and ligated (III) molecules are consistent with

Table I: Thermodynamic Data<sup>a</sup>

	structure	<i>f</i> (conc)	$\Delta H^\circ$ (kcal/mol) <sup>b</sup>	$\Delta S^\circ$ (eu)	$\partial T_m / \partial \log [\text{Na}^+]$ (°C)	$\Delta i$ (phosphate <sup>-1</sup> )	$\Delta i$ (phosphate in duplex) <sup>-1</sup>
I		no	55	174	13.5	0.065	0.109
II		no	51	159	15.6	0.066	0.107
III		no	68	192	8.0	0.037	0.059
IV		no	54	173	11.5	0.057	0.087
V		no	45	143	13.4	0.057	0.086
VI	GGAATTCCCTTAAGG	yes	58	—	12.3	0.096	0.096

<sup>a</sup>The  $\Delta H^\circ$ ,  $\Delta S^\circ$ , and  $\Delta i$  data listed for structures I–V are averages over all added salt concentrations studied between 0.0 and 0.3 M NaCl. The deviation of an individual measurement from these average values never exceeds 5%. <sup>b</sup>The enthalpies reported in this column are average van't Hoff transition enthalpies derived from normalized optical melting curves, except for that of the octamer (VI) which was calorimetrically determined (Patel et al., 1982).

the formation of B-like structures at low temperatures (Ts'o, 1974; Cantor & Schimmel, 1980). Furthermore, the temperature-dependent CD spectra of these three molecules are similar to one another and similar to the CD melting profiles of the corresponding 24-mer sequences (Erie et al., 1987). Significantly, for each species (I, II, and III) the temperature-dependent CD spectra exhibit an isoelliptic point at 233 nm. This observation is consistent with a two-state equilibrium for the thermally induced order-disorder transitions of molecules I, II, and III (Ts'o, 1974).

**Calorimetry.** We determined the calorimetric transition enthalpy ( $\Delta H_{\text{cal}}$ ) for the unphosphorylated 26-mer structure (I) by integrating the area under the experimental heat capacity versus temperature curve. On the basis of four measurements, we obtained an average transition enthalpy of 54 kcal/mol of strand. We also calculated the corresponding van't Hoff transition enthalpy ( $\Delta H_{\text{cal}}^{\text{H}}$ ) of I by analyzing the shape of each calorimetric transition curve using previously described methods (Breslauer et al., 1975; Marky et al., 1983; Breslauer, 1986; Marky & Breslauer, 1987). Significantly, the average van't Hoff transition enthalpy calculated from the shapes of the four calorimetric curves also is equal to 54 kcal/mol. This equality between the van't Hoff and the calorimetric transition enthalpies indicates that the melting transition of I occurs in a two-state manner (Sturtevant, 1987; Breslauer, 1986; Marky & Breslauer, 1987). Unfortunately, we could not conduct the corresponding calorimetric measurements on the phosphorylated (II) and the ligated (III) forms of the 26-mer since neither derivative was produced in sufficient quantities for calorimetric measurements. With the reasonable assumption that structures II and III also melt in a two-state manner (an assumption consistent with the isoelliptic point in the temperature-dependent CD spectra), we employed a van't Hoff analysis to obtain the requisite thermodynamic data from the UV melting curves.

**Salt-Dependent UV Melting Studies.** The melting temperatures ( $T_m$ ) and van't Hoff transition enthalpies ( $\Delta H_{\text{H}}$ ) were derived from normalized optical melting profiles of the unphosphorylated (I), phosphorylated (II), and ligated (III)

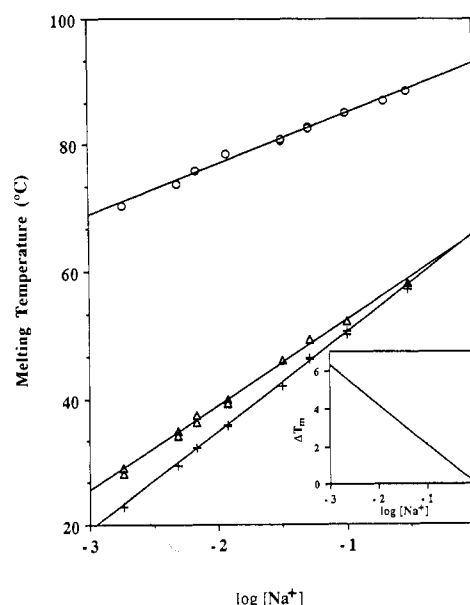


FIGURE 2: Melting temperature,  $T_m$ , versus  $\log [\text{Na}^+]$  profiles for the unphosphorylated ( $\Delta$ ), phosphorylated ( $+$ ), and ligated ( $\circ$ ) forms of the 26-mer sequence, TTAAT<sub>5</sub>GGAATTCCT<sub>5</sub>GGAA. The insert is a plot of the difference in melting temperatures,  $\Delta T_m$ , between the phosphorylated and unphosphorylated sequences as a function of sodium chloride concentration.

26-mers. For all three molecules at all salt concentrations studied, the melting curves are monophasic (see paragraph at end of paper regarding supplementary material). The average thermodynamic values obtained from these melting curves are listed in Table I. For each species, the dependence of the melting temperature on sodium ion concentration ( $\partial T_m / \partial \log [\text{Na}^+]$ ) also was determined from the slopes of the lines shown in Figure 2. These data ( $T_m$ ,  $\Delta H_{\text{H}}$ , and  $\partial T_m / \partial \log [\text{Na}^+]$ ) were substituted into eq 1 to calculate the change in the thermodynamic degree of ion dissociation upon denaturation,  $\Delta i$ . The resulting average  $\Delta i$  values also are listed in Table I along with other pertinent data. For comparative purposes,

the table includes the thermodynamic data for the corresponding 24-mer molecules (IV and V) (Erie et al., 1987) and the common core duplex (VI) (Patel et al., 1982). Inspection of the data listed in Table I and plotted in Figure 2 reveals several significant features:

(1) For all salt concentrations studied, ligation results in an increase in the thermal stability ( $T_m$ ) of the 26-mer, relative to its unligated counterparts (III vs I and II) (see Figure 2). This ligation-induced increase in  $T_m$  is enthalpic in origin (Table I).

(2) The magnitude of the change in the degree of ion dissociation,  $\Delta i$ , that accompanies the thermally induced transition of the structure formed by the 26-mer (I) is not altered by 5'-phosphorylation (II). Significantly, however, the magnitude of  $\Delta i$  is greatly decreased by ligation of the 26-mer molecule (compare  $\Delta i$  data for II vs that for III in Table I).

(3) For all three species (I, II, and III), the  $T_m$ 's are a linear function of  $\log [\text{Na}^+]$  (see Figure 2). However, the specific values of  $\partial T_m / \partial \log [\text{Na}^+]$  listed in Table I are different for each species.

(4) At low salt concentrations, 5'-phosphorylation decreases the thermal stability ( $T_m$ ) of the structure formed by the unligated 26-mer (I vs II) (see Figure 2). This phosphorylation-induced decrease in thermal stability is enthalpic in origin (Table I).

(5) The influence of the phosphorylation-induced decrease in  $T_m$  becomes less with increasing salt concentration. In fact, as emphasized by the insert in Figure 2, the  $T_m$ 's of the unphosphorylated (I) and the phosphorylated (II) unligated sequences are approximately equal ( $\Delta T_m \approx 0$ ) at 1.0 M  $[\text{Na}^+]$ .

(6) The  $T_m$ 's for all three forms of the 26-mer (I, II, and III) are independent of oligomer concentration (data not shown).

We propose below possible explanations for these observations.

## DISCUSSION

In the following sections, we discuss the melting behavior of the ligated 26-mer sequence (III) and we compare it with the melting of its unligated, phosphorylated precursor (II) (hereafter referred to as the unligated molecule). This comparison allows us to determine quantitatively the effect of closing the central duplex nick and producing a covalently closed, single-stranded, circular final state.

**Ligation Increases the Thermal Stability and the Transition Enthalpy of the 26-mer.** Inspection of Figure 2 reveals that ligation of the nicked 26-mer (II) causes a large increase in thermal stability ( $\Delta T_{m, \text{ligated-unligated}} = 25\text{--}50^\circ\text{C}$ ). The data in Table I show that this ligation-induced increase in thermal stability is exclusively enthalpic in origin ( $\Delta \Delta H_{vH, \text{ligated-unligated}} = +17 \text{ kcal/mol}$ ). The exact magnitude of this difference depends on salt concentration since the transition enthalpy of structure II exhibits a weak dependence on  $\log [\text{Na}^+]$  similar to that of its corresponding 24-mer (Erie et al., 1987). Significantly, however, the magnitude of this salt effect on  $\Delta H_{vH}$  is small compared with the large influence of ligation on  $\Delta H_{vH}$ .

**Charge Density of a Linear versus a Circular Single-Stranded 26-mer.** The  $\partial T_m / \partial \log [\text{Na}^+]$  data in Table I exhibit a reduced salt-dependence for the transition temperature of the ligated molecule (III) relative to its unligated precursor (II) ( $8.0^\circ\text{C}$  versus  $15.6^\circ\text{C}$ ). Strictly speaking, the values of  $\Delta i$  should be compared rather than  $\partial T_m / \partial \log [\text{Na}^+]$  since the dependence of  $T_m$  on counterion concentration is a function not only of the number of counterions released upon denaturation,  $\Delta i$ , but also on the transition enthalpy,  $\Delta H^\circ$  (Record

et al., 1978; Erie et al., 1987).

Inspection of the data in the penultimate column of Table I reveals that  $\Delta i$  equals 0.066 for the unligated 26-mer (II) and only 0.037 for the ligated 26-mer (III). This decrease in ion release for the ligated 26-mer structure (III) relative to its unligated counterpart (II) may reflect a reduced ion association for the initial double-stranded state of the ligated 26-mer (III) or an increased ion association for the final single-stranded state of the melted ligated molecule (III). In the unligated structure (II), the two hairpin halves of the double-stranded molecule can, in principle, rotate about the phosphodiester bond opposite the nick to relieve electrostatic repulsions. Such a skewed dumbbell conformation would exhibit a lower charge density than a rotamer with a continuous core duplex (Erie et al., 1987). Since ligation removes this rotational degree of freedom, we propose that the native state of the ligated 26-mer (III) will have a charge density that is *not less* than that of the unligated structure (II). For this reason, we propose that the decrease in ion release we observe upon ligation reflects an increased ion association in the final "circular", single-stranded state of the ligated 26-mer (III) relative to the final "linear", single-stranded state of the unligated 26-mer (II). If our assumption is correct that the native (initial) states of the unligated (II) and ligated (III) molecules have similar charge densities, then, on the basis of our  $\Delta i$  data, the melted circular, single-stranded state of 26 residues should have approximately 45% [ $= (1 - 0.037/0.066) \times 100$ ] more counterions associated with it relative to the melted linear, single-stranded state of 26 residues. This result suggests that a small circular single strand may have a significantly greater charge density than the corresponding linear single strand. Such a result should be of importance in developing a quantitative understanding of the molecular forces that dictate local domain melting within DNA polymers, an event that may be important in recognition and control mechanisms of gene expression (von Hippel & Berg, 1987).

**Ligation Results in an Increase in the Entropy of Denaturation.** We observe a large increase in transition entropy upon ligation [ $\Delta \Delta S_{\text{ligated-unligated}}^\circ = +33 \text{ cal}/(\text{mol} \cdot \text{K})$ ] (Table I). In general, a difference in the transition entropies of two structures ( $\Delta \Delta S_{\text{obs}}^\circ$ ) will reflect potential contributions from differential changes in counterion "binding" ( $\Delta \Delta S_{[M^+]}^\circ$ ), conformational entropy ( $\Delta \Delta S_{\text{conf}}^\circ$ ), and solvation ( $\Delta \Delta S_{\text{solv}}^\circ$ ). In other words,  $\Delta \Delta S_{\text{obs}}^\circ = \Delta \Delta S_{[M^+]}^\circ + \Delta \Delta S_{\text{conf}}^\circ + \Delta \Delta S_{\text{solv}}^\circ$ . In an effort to determine the relative contributions that each of these components make to  $\Delta \Delta S_{\text{obs}}^\circ$ , we will focus our initial attention on the  $\Delta \Delta S_{[M^+]}^\circ$  term. For the ligated species (III), we observe a decrease in the number of thermodynamically bound counterions released upon denaturation,  $\Delta i$ , relative to the unligated species. Since the entropy of counterion release,  $\Delta S_{[M^+]}^\circ$ , is proportional to  $\Delta i$ , this result corresponds to a decrease in the transition entropy of the ligated molecule relative to the unligated molecule. Consequently, counterion release should make a negative contribution to the differential change in transition entropy,  $\Delta \Delta S_{\text{obs}}^\circ$ , between the ligated (III) and unligated (II) species. In other words,  $\Delta \Delta S_{[M^+]}^\circ < 0$ .

We now will focus our attention on the contributions from the  $\Delta \Delta S_{\text{conf}}^\circ$  term. Ligation causes a reduction in the conformational entropy of both the initial (double-stranded) and final (denatured) states of the dumbbell. We propose that this reduction in conformational entropy is greater in the denatured than in the native state since the native form of the unligated molecule already is significantly constrained. Specifically, in the final melted state, loop closure satisfies two structural constraints: (1) the 5' and 3' ends of the single-stranded

molecule are separated by a single bond distance; (2) the 3'-OH and 5'-P are oriented so that they form proper P-O-C and P-O-P valence bond angles. By contrast, formation of the phosphodiester bond in the initial double-stranded state of the dumbbell removes only the rotational degree of freedom about the phosphodiester bond opposite the nick, since the ends of the rotamer which has an untwisted, continuous core duplex already will exhibit the proper geometry for bond formation. Consequently, we propose that upon ligation the conformational entropy also makes a negative contribution to the overall change in transition entropy. In other words,  $\Delta\Delta S_{\text{conf}}^{\circ} < 0$ .

In the discussion presented above, we argue that counterion release and conformational entropy both make negative contributions to the ligation-induced change in transition entropy ( $\Delta\Delta S_{\text{obs}}^{\circ}$ ). Thus, only entropy changes associated with solvent release ( $\Delta\Delta S_{\text{sol}}^{\circ}$ ) remain to account for the observed increase in transition entropy upon ligation ( $\Delta\Delta S_{\text{obs}}^{\circ} > 0$ ). This increase in solvent release upon melting could result from a more highly hydrated duplex state or a less hydrated single-stranded state of the ligated molecule (III) relative to its unligated counterpart (II). By analogy with solvent accessibility studies on tRNAs (Thiyagarajan & Ponnuswamy, 1979; Alden & Kim, 1979), we suggest that the interior of the melted single-stranded circle is solvent accessible. However, even if the melted ligated molecule is solvent accessible, its local solvent environment may be different from that of the linear melted species, thereby affecting the transition entropy. It is difficult, however, to predict a priori the direction of this change, since it is not clear which of the denatured species (ligated or unligated) might be more hydrated. Nevertheless, the single-stranded states of both molecules should be very flexible, thereby inhibiting the formation of extended hydrogen-bonded networks (Westhof, 1987; H. Berman, personal communication). For this reason, we propose that the differences in transition entropy ( $\Delta\Delta S_{\text{obs}}^{\circ}$ ) that we observe primarily reflect a more hydrated initial state of the ligated species (III) relative to its unligated counterpart (II).

We propose below several ligation-induced changes in the dumbbell to rationalize the increase in the transition entropy that we measure for the ligated species. For this purpose, we assume that differences in solvation for the ligated and unligated sequences exist predominately in the double-stranded, initial states.

(1) After ligation, the dumbbell no longer has the freedom to rotate about the phosphodiester bond opposite the gap, thus producing a more rigid structure. It seems reasonable to suggest that water can more effectively form cooperative, hydrogen-bonded networks around such a rigid DNA structure (Saenger et al., 1986; Westhof, 1987; Subramanian et al., 1988; Berman et al., 1988; H. Berman, personal communication). In such a model, the ligated initial state will be more hydrated than its more flexible, unligated counterpart. This differential solvation would yield a more positive transition entropy for the ligated 26-mer.

(2) The AATT duplex core present in the 26-mer is postulated to possess a spine of hydration in the minor groove (Drew & Dickerson, 1981; Kopka et al., 1983). Rotation of the two hairpin halves about the central phosphodiester bond would interrupt the AATT continuity in the minor groove, thereby disrupting the spine of hydration. Consequently, the minor groove of the ligated molecule (III) should be more hydrated than the minor groove of the unligated molecule (II).

**Hairpin Electrostatics and Hydration.** Inspection of the data in Table I reveals that the unphosphorylated and the phosphorylated 26-mers (I and II) exhibit similar salt-de-

pendent melting behaviors ( $\partial T_m / \partial \log [\text{Na}^+]$  and  $\Delta i$ ). The  $\Delta i$  values in the penultimate column were calculated by assuming that the loop phosphates behave electrostatically as double strands, whereas the  $\Delta i$  values in the last column were calculated by assuming that the loop phosphates behave electrostatically as single strands. The close agreement between the  $\Delta i$  values in the last column and the  $\Delta i$  value of the corresponding core duplex,  $[\text{d}(\text{GGAATTCC})]_2$  (VI), suggests that the phosphates in the hairpin loops behave electrostatically as denatured coils. A similar conclusion was reached for the looped regions of the corresponding 24-mer sequences IV and V (Erie et al., 1987). These results may reflect greater phosphate distances in the loops compared to the duplex region.

Alternatively, the  $\Delta i$  values we observe may reflect different local environments within the hairpin loops relative to the double-stranded regions. Such differences in local environments may result from greater solvent accessibilities in hairpin loops relative to double-stranded regions (Thiyagarajan & Ponnuswamy, 1979; Alden & Kim, 1979). If the interiors of the hairpin loops in our dumbbell structures are solvent accessible, then the loop phosphates may be interacting through a dielectric constant close to that of water ( $\approx 80$  D). By contrast, the dielectric constant within double-stranded DNA appears to be substantially less than that of water (Jin & Breslauer, 1988), thereby suggesting that the phosphates within the duplex region of our dumbbell structures may be interacting through a medium with a dielectric constant less than 80 D. Since the electrostatic energy is inversely proportional to the dielectric constant, and for low molecular weight DNA the amount of ion association appears to be related to the electrostatic energy (Manning, 1969), the phosphate distances in the loops could be similar to the phosphate distances in the duplex region and still have fewer ions associated with them. It also has been suggested that molecular shape may significantly affect phosphate-phosphate interactions in DNA due to dielectric differences in neighboring local environments (Troll et al., 1986; Jayaram et al., 1989). For example, Troll et al. demonstrated, using a clay model of DNA and an electrolyte tank, that the low dielectric cavity in the minor groove significantly enhances phosphate interactions on the same side of the DNA and reduces those on opposite sides. Thus, the flexibility and molecular geometry of the hairpin loops may be such that the phosphate interactions in the loops are reduced relative to those in the double strand. On the basis of the above discussions, the  $\Delta i$  data we have obtained can be rationalized in terms of a model that evokes greater phosphate separations, increased solvent accessibility, and/or different molecular geometry in the hairpin loops relative to the double-stranded regions.

**Loop Size and Ligation.** We previously reported that the 24-mer (V) was resistant to ligation over a broad range of temperatures and solution conditions. By contrast, in this work, we have successfully ligated the 26-mer sequence (II), a structure which only differs from the 24-mer by the addition of one thymine residue per hairpin loop. For the 24-mer structure (V), we proposed that loops of four thymine residues may constrain the duplex region of the dumbbell causing the 5' and 3' ends at the nick to be twisted relative to the helical axis and therefore to be out of phase (Erie et al., 1987). Such conformations may account for the resistance of the 24-mer double-hairpin structure to ligation, since the 3'-OH and 5'-P would no longer be collinear. The additional residue in each hairpin loop of the proposed dumbbell-shaped structure of the 26-mer (II) may permit the terminal residues at the nick to assume a collinear conformation, thereby facilitating ligation.

Our successful ligation of the 26-mer is consistent with this interpretation.

#### ACKNOWLEDGMENTS

We thank Dr. Helen M. Berman and Dr. Gerald S. Manning for helpful discussions and Dr. Barbara Gaffney for the synthesis and purification of the 26-mer.

#### SUPPLEMENTARY MATERIAL AVAILABLE

Figure depicting normalized UV melting profiles for the phosphorylated unligated (II), the unphosphorylated unligated (I), and the phosphorylated ligated (III) 26-mer molecules (1 page). Ordering information is given on any current masthead page.

**Registry No.** I, 118016-93-6; II, 117982-70-4; III, 117982-69-1; IV, 117982-67-9; V, 117982-68-0; VI, 70755-49-6.

#### REFERENCES

- Alden, G. C., & Kim, S. M. (1979) *J. Mol. Biol.* **132**, 411-434.
- Baldwin, R. L. (1971) *Acc. Chem. Res.* **4**, 265-272.
- Benight, A. S., Schurr, J. M., Flynn, P. F., Reid, B. R., & Wemmer, D. E. (1988) *J. Mol. Biol.* **200**, 377-399.
- Berman, H. M., Sowri, A., Ginell, S., & Beveridge, D. (1988) *J. Biomol. Struct. Dyn.* **5**, 1101-1110.
- Breslauer, K. J. (1986) in *Thermodynamic Data for Biochemistry and Biotechnology* (Hinz, H.-J., Ed.) Chapter 15, pp 402-427, Springer-Verlag, New York.
- Breslauer, K. J., Sturtevant, J. M., & Tinoco, I., Jr. (1975) *J. Mol. Biol.* **99**, 549-565.
- Breslauer, K. J., Frank, R., Blocker, H., & Marky, L. A. (1986) *Proc. Natl. Acad. Sci. U.S.A.* **83**, 3746-3750.
- Cantor, C. R., & Schimmel, P. R. (1980) *Biophysical Chemistry*, Vol. III, Chapter 22, pp 1109-1124, Freeman, San Francisco.
- Cantor, C. R., Warshaw, M. M., & Shapiro, H. (1970) *Biopolymers* **9**, 1059-1077.
- Drew, H. R., & Dickerson, R. E. (1981) *J. Mol. Biol.* **151**, 535-556.
- Erie, D., Sinha, N., Olson, W., Jones, R., & Breslauer, K. (1987) *Biochemistry* **26**, 7150-7159.
- Gaffney, B. L., & Jones, R. A. (1988) *Tetrahedron Lett.* **29**, 2619-2622.
- Germann, M. W., Schoenwaelder, K.-H., & van de Sande, J. H. (1985) *Biochemistry* **24**, 5698-5702.
- Jayaram, B., Sharp, K. A., & Honig, B. (1989) *Biopolymers* (in press).
- Kopka, M. L., Fratini, A. V., Drew, H. R., & Dickerson, R. E. (1983) *J. Mol. Biol.* **163**, 129-146.
- Lilley, D. M. (1986) *Nature (London)* **320**, 487-488.
- Manning, G. S. (1969) *J. Chem. Phys.* **51**, 924-933.
- Marky, L. A., & Breslauer, K. J. (1987) *Proc. Natl. Acad. Sci. U.S.A.* **84**, 4359-4363.
- Marky, L. A., Blumenfeld, K. S., Kozlowski, S., & Breslauer, K. J. (1983) *Biopolymers* **22**, 1247-1257.
- Müller, U. R., & Fitch, W. M. (1982) *Nature (London)* **298**, 582-585.
- Patel, D. J., Kozlowski, S. A., Marky, L. A., Rice, J. A., Broka, C., Itakura, K., & Breslauer, K. J. (1982) *Biochemistry* **21**, 451-455.
- Pheiffer, B. H., & Zimmerman, S. B. (1983) *Nucleic Acids Res.* **11**, 7853-7871.
- Record, M. T., Jr., Anderson, C. F., & Lohman, T. M. (1978) *Q. Rev. Biophys.* **11**, 103-178.
- Saenger, W., Hunter, W. N., & Kennard, O. (1986) *Nature (London)* **324**, 385-388.
- Scheffler, I. E., Elson, E. L., & Baldwin, R. L. (1970) *J. Mol. Biol.* **48**, 145-171.
- Streisinger, G., Ikada, Y., Emrich, J., Newton, J., Tsugita, A., Terzaghi, E., & Inouye, M. (1966) *Cold Spring Harbor Symp. Quant. Biol.* **31**, 77.
- Sturtevant, J. M. (1987) *Annu. Rev. Phys. Chem.* **38**, 463-488.
- Subramanian, P. S., Ravishanker, G., & Beveridge, D. L. (1988) *Proc. Natl. Acad. Sci. U.S.A.* **85**, 1836-1840.
- Thiyagarajan, P., & Ponnuswamy, P. K. (1979) *Biopolymers* **18**, 2233-2247.
- Troll, M., Roitman, D., Conrad, J., & Zimm, B. H. (1986) *Macromolecules* **19**, 1186-1194.
- Ts'o, P. O. P. (1974) in *Basic Principles in Nucleic Acid Chemistry* (Ts'o, P. O. P., Ed.) pp 305-469, Academic, New York.
- Von Hippel, P. H., & Berg, O. G. (1987) in *DNA-Ligand Interactions* (Guschlbauer, W., & Saenger, W., Eds.) pp 159-171, Plenum, New York.
- Wemmer, D. E., & Benight, A. S. (1985) *Nucleic Acids Res.* **13**, 8611-8620.
- Westhof, E. (1987) *Int. J. Biol. Macromol.* **9**, 186-192.
- Yager, T. D., & von Hippel, P. H. (1987) in *Cellular and Molecular Biology* (Neidhardt, F., et al., Eds.) pp 1241-1275, American Society of Microbiology, Washington, DC.
- Zimmerman, S. B., & Pheiffer, B. H. (1983) *Proc. Natl. Acad. Sci. U.S.A.* **80**, 5856-5858.